Spin-polarized scanning tunnelling microscopy with detection of polarized luminescence emerging from a semiconductor tip

1997 J. Phys.: Condens. Matter 9 5697

(http://iopscience.iop.org/0953-8984/9/27/003)

J. Phys.: Condens. Matter **9** (1997) 5697–5707. Printed in the UK PII: S0953-8984(97)80559-0

Spin-polarized scanning tunnelling microscopy with detection of polarized luminescence emerging from a semiconductor tip

R Laiho and H J Reittu†

Wihuri Physical Laboratory, University of Turku, 20014 Turku, Finland

Received 2 January 1997, in final form 14 March 1997

Abstract. A variant of scanning tunnelling microscopy with spin-resolving properties, based on observation of circularly polarized luminescence from a semiconductor tip, is suggested. The method is analysed using a three-step model of electron transport, including tunnelling from a ferromagnetic sample to the tip through the vacuum gap, ballistic transport through the band-bending region of the tip subsurface and radiative recombination with holes in the semiconductor bulk. The tunnelling of spin-polarized electrons is treated with the transfer-Hamiltonian method. Then the model reveals a close connection between the degree of circular polarization of the light and the local spin polarization of the sample surface: namely, by making measurements with photons propagating in three non-collinear directions it would be possible to obtain a complete map of the distribution of surface spins with high spatial resolution without affecting the magnetization of the surface. The possibility of practical realization of such experiments is discussed.

1. Introduction

The invention of scanning probe microscopies (SPMs), including scanning tunnelling microscopy (STM) [1] and atomic force microscopy (AFM) [2], has allowed studies of solid surfaces down to atomic scale. Recently several authors have investigated the possibilities of applying SPM to reveal surface magnetic properties with a high lateral resolution [3–19]. These techniques are referred as spin-polarized scanning tunnelling microscopy (SPSTM), magnetic force microscopy (MFM) [18, 19] and spin-polarized atomic force microscopy (SPAFM) [16]. The feasibility of magneto-optical near-field imaging with a photosensitive semiconductor tip has also been tested [20]. In addition, use of a ferromagnetic or an antiferromagnetic metallic tip as the source of spin-polarized electrons in SPSTM is supported by theory [3, 21] and by experiments [4, 6] as well.

The stray magnetic field of a ferromagnetic tip may disturb the sample magnetization. Then it is difficult to distinguish spin-dependent features from other contributions of the surface. To circumvent this problem use of a semiconducting tip (e.g. GaAs) where spin-polarized conduction band (c-band) electrons can be obtained by pumping with circularly polarized light has been proposed [8, 11, 15–17]. A convenient feature is that the spins of the electrons in this kind of tip can be reversed by switching the helicity of the pumping light between right- and left-hand circular polarization. This approach is supported by ordinary STM experiments [10, 12, 14] showing that it is possible to obtain atomically resolved

---

† E-mail address: hannu.reittu@utu.fi

0953-8984/97/275697+11$19.50

topographic surface images with an STM tip prepared from highly doped p-GaAs. Spin-dependent tunnelling current has also been detected in a thin Co–Al_2O_3–GaAs ferromagnet to semiconductor film junction [22].

Under pumping with circularly polarized light spin-polarized electrons are created in the subsurface region of the GaAs tip within a depth of the order of 1 μm [23]. These electrons can tunnel to the sample only if they diffuse to the tip apex during their lifetime. On the other hand illumination can reduce the resolution due to enhanced thermal fluctuations in the tip. The energy bands of a tip made of a p-type III–V semiconductor are usually bent downward in the sub-surface region due to the presence of surface states capable of trapping carriers. This gives rise to a sub-surface electric field and the surface photovoltage effect SPV [24] since the minority carriers are accelerated by the field toward the surface and the majority carriers toward the bulk. Such surface states are likely to be present even in a well controlled environment due to strongly reduced crystallographic symmetry of the tip [15]. Although spin-polarized electrons can reach the tip apex, they may not tunnel to the sample but are captured by defects or surface states. This is because such capture is much more probable than tunnelling to the sample [15]. Only if the spin polarization of the trapped electrons is conserved is the tunnelling current to a magnetic sample spin dependent [15]. In the reverse tunnelling, from the sample to the tip, the situation is analogous. Since the states at the conduction band (c-band) edge of the tip are empty the tunnelling current from the sample to these states is spin-independent.

Using a ferromagnetic Ni tip and a p-GaAs Zn-doped 10^{19} cm^{-3} sample, emission of circularly polarized light induced by injection of spin-polarized electrons from the tip to the sample has been observed [5]. Similar studies of STM-excited luminescence but without analysis of the polarization have been carried out by several authors [25, 26]. In practice it is difficult to define well the polarization of the electrons emitted from a magnetic tip since it depends on the circumstances (orientation of the lattice facets etc) of the tip apex. Recently it has been established that localized plasma modes can decay radiatively in an STM junction [27–30]. Another possible mechanism that is effective on dielectric surfaces is tunnelling of electrons to empty higher states from which they can fall to lower empty states emitting a photon [31]. Such radiation was found to be partially circularly polarized [30], a circumstance that allows in principle investigation of surface magnetization.

Here we discuss a variant of SPSTM where a semiconductor tip is utilized and the restrictions with optically pumped tips mentioned above can be avoided as well as the stray magnetic field emerging from a magnetized tip. The proposed method is based on observation of circularly polarized light from the tip forming a tunnel junction with a magnetic surface. Such a configuration is opposite to the one [5] where a metallic ferromagnet (Ni) was used as the tip and the sample was GaAs. However, the physical origin of the electron spin polarization is the same in both cases and our theoretical analysis can be used to interpret the results obtained in [5], too.

2. The degree of spin polarization of the injected electrons

Suppose that the Fermi level of a ferromagnetic sample lies above the c-band of a p-type semiconductor (e.g. p-GaAs) tip with a clean surface. Then the elastic tunnelling of spin-polarized Fermi electrons from the sample takes place mainly to the c-band states of the tip and not to the surface states which have energies in the band gap of the semiconductor (see figure 1). After tunnelling a substantial fraction of the electrons penetrate ballistically through the band-bending region and enter the bulk of the semiconductor, thermalizing to the c-band minimum. In the bulk the electrons recombine with holes, producing circularly

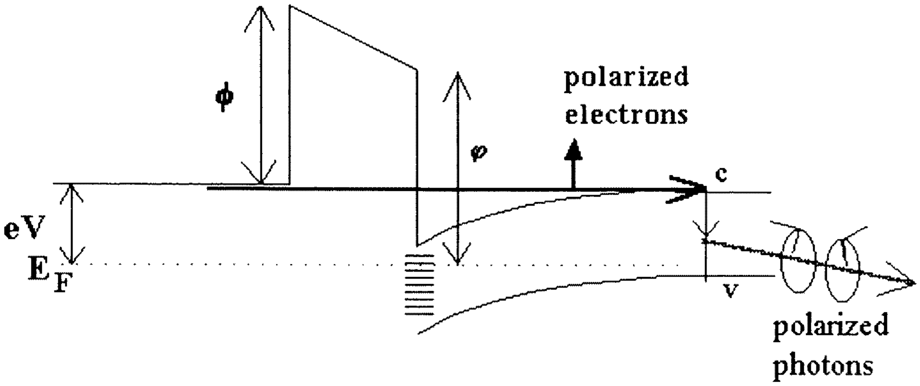

Figure 1. The tunnelling barrier of the proposed spin-sensitive STM with detection of circularly polarized luminescence from a semiconductor tip. Some of the spin-polarized electrons tunnelling from left to right pass the subsurface region of the semiconductor tip where the energy bands (c and v) are bent due to surface states (vertical lines). Then they diffuse into the interior of the tip where they are recombined with equilibrium holes producing photons. The bias voltage, V, lifts the Fermi level, E_F, of the ferromagnet just above the semiconductor c-band (c) edge to ensure effective injection of spin-polarized electrons. Work functions of the ferromagnetic sample and the semiconductor tip are denoted as ϕ and φ, respectively.

polarized luminescence. The degree of the circular polarization is defined as

$$A = (I_+ - I_-)/(I_+ + I_-) \tag{1}$$

where I_+ and I_- are the intensities of the right- and the left-hand circularly polarized components of the light, respectively. To describe the degree of polarization of the luminescence we adopt the three-step model [23]: (i) vacuum tunnelling of the spin-polarized electrons between the ferromagnetic sample and the semiconductor tip; (ii) transport of the electrons to the bulk of the semiconductor and (iii) radiative recombination of the injected electrons with holes (see figure 2).

Vacuum tunnelling of the spin-polarized electrons can be analysed with the Bardeen transfer-Hamiltonian method [32], expressing the Bardeen tunnelling matrix element as

$$M_\sigma = \frac{-\mathrm{i}\hbar^2}{2m_e}\int_s (\chi_\sigma^*\nabla\psi_\sigma - \psi_\sigma\nabla\chi_\sigma^*)\,\mathrm{d}\boldsymbol{S} \tag{2}$$

where $\mathrm{d}\boldsymbol{S}$ is a differential vector element pointing along the normal of a separation surface $\boldsymbol{S}$ located in the middle of the vacuum gap between the tip and the sample. χ_σ and ψ_σ are the wave functions of the electrons with spin projection $\sigma(\uparrow$ or $\downarrow)$ in the tip and in the sample, respectively. The coordinate-dependent parts of the tip wave functions $\chi\uparrow$ and $\chi\downarrow$ are assumed to be identical. In what follows the electrons with the spin projection σ are called 'σ-electrons'.

The transition rate of an electron from state ψ_σ to state χ_σ per unit time is given by Fermi's golden rule

$$w_\sigma = (2\pi/\hbar)|M_\sigma|^2\delta(E_\chi - E_\psi) \tag{3}$$

where E_χ and E_ψ are the energy eigenvalues of the wave functions involved. The maximum energy of the electrons injected above the bottom of the c-band, E_c, is $E = eV - E_c$ where V is the tunnelling voltage applied to the sample. Increasing polarization is expected when E diminishes [5, 8]. Then the highest degree of the electron spin polarization (ESP) is

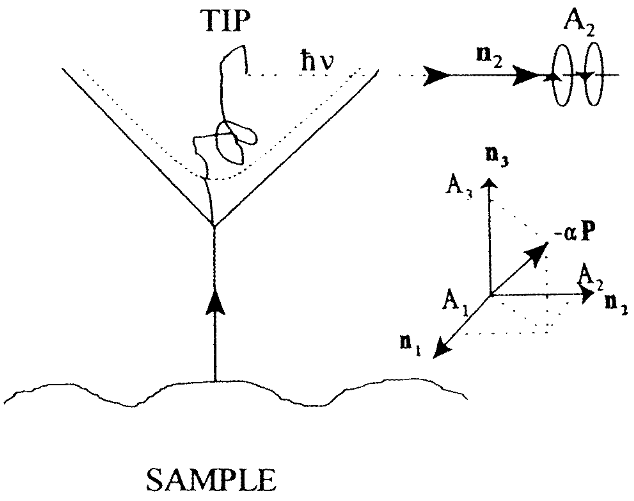

Figure 2. An illustration of the three-step model for spin-polarized STM. Spin-polarized electrons tunnel from the sample through the vacuum gap into the tip. Then they penetrate ballistically the band-bending region (between the tip surface and the dotted line) and diffuse to the interior of the tip where they are recombined with holes (p-type tip material is assumed) producing circularly polarized photons with energy $\hbar\nu$. The degree of circular polarization of the light, A_i, propagating along the vector $\boldsymbol{n}_i$ is proportional to the projection of the spin polarization vector $\boldsymbol{P}$ of the sample surface in this same direction. By measuring A_i, corresponding to three noncollinear directions $(\boldsymbol{n}_1, \boldsymbol{n}_2, \boldsymbol{n}_3)$, the vector $-\alpha\boldsymbol{P}$ where α is a constant $(0 \leqslant \alpha \leqslant 1)$ is completely determined.

obtained when the Fermi level of the ferromagnet is situated just above the bulk value of the c-band edge of the semiconductor, i.e. $eV - E_c \gtrsim 0$ (see figure 1). Then the total rate of the spin-polarized electron transfer is to a good approximation

$$C_\sigma \propto N_\sigma(E_F)|M_\sigma|^2 \tag{4}$$

where N_σ is the density of the σ-electron states at the Fermi level of the sample. After tunnelling some of these electrons cross the band-bending region and diffuse to the bulk of the tip, thermalizing to the band minimum. During this process the spin polarization is partly lost via spin relaxation characterized by the spin-relaxation time τ_s.

The generation rate, g_σ, of the σ-electrons in the tip is proportional to C_σ in (4). If their number is denoted by n_σ the rate equation of the total number of the minority carriers can be written as

$$\mathrm{d}(n_\uparrow + n_\downarrow)/\mathrm{d}t = g_\uparrow + g_\downarrow - (1/\tau)(n_\uparrow + n_\downarrow) \tag{5}$$

where $1/\tau$ is the electron recombination rate. Taking into account the spin relaxation the difference between the numbers of electrons with the two spin projections takes the form

$$\mathrm{d}(n_\uparrow - n_\downarrow)/\mathrm{d}t = g_\uparrow - g_\downarrow - (1/\tau)(n_\uparrow - n_\downarrow) - (1/\tau_s)(n_\uparrow - n_\downarrow). \tag{6}$$

Under stationary conditions the time derivatives in (5) and (6) are zero. Using (4) as well as the relation $g_\sigma \propto C_\sigma$ we obtain an expression for the spin polarization of the tip electrons in the form

$$\boldsymbol{P} \equiv \frac{n_\uparrow - n_\downarrow}{n_\uparrow + n_\downarrow}\boldsymbol{h} = \frac{T}{\tau}\boldsymbol{P}_I \tag{7}$$

where $\boldsymbol{h}$ is a unit vector along the mean value of the spin,

$$P_I = |\boldsymbol{P}_I| = (g_\uparrow - g_\downarrow)/(g_\uparrow + g_\downarrow) = (N_\uparrow|M_\uparrow|^2 - N_\downarrow|M_\downarrow|^2)/(N_\uparrow|M_\uparrow|^2 + N_\downarrow|M_\downarrow|^2) \tag{8}$$

and

$$1/T = 1/\tau + 1/\tau_s. \tag{9}$$

The physical meaning of P_I is discussed in connection with (16)–(19). To achieve a large value of P, T/τ should not be too small. This is possible e.g. in highly doped p-GaAs tip material where τ_s can be greater than τ [33]. The ratio τ_s/τ may vary in a wide range depending on temperature and concentration of the impurities, defects and the majority carriers.

The spin-density matrix of the injected and thermalized electrons can be parametrized as

$$\boldsymbol{\rho} = \tfrac{1}{2}(\mathsf{I} + \boldsymbol{P}\cdot\boldsymbol{\sigma}) \tag{10}$$

where I is the unit 2×2 matrix and $\boldsymbol{\sigma}$ are the Pauli matrices. Thus the mean value of the spin $\langle s\rangle = S_p(\sigma\rho)$ is

$$\langle\boldsymbol{s}\rangle = \tfrac{1}{2}\boldsymbol{P}. \tag{11}$$

For the next we consider radiative recombination of the electrons with equilibrium holes in GaAs where the bottom of the c-band and the top of the v-band are located at the centre of the Brillouin zone (Γ-point) making direct-gap transitions of high efficiency possible. The c-band is twofold degenerate with spin. The v-band consists of three twofold-degenerate subbands, one of which is split off from the others by the spin–orbit splitting Δ. At high p-doping of the tip material its Fermi level is close to the top of the v-band. Thus a considerable number of holes is available for radiative recombination with the minority carriers injected from the sample. It is just this luminescence which we suggest to be utilized in a spin-polarized scanning tunnelling microscope.

The parameter A defined by (1) is related to the mean spin of the minority carriers by [33]

$$A = -2\alpha\langle\boldsymbol{s}\rangle\cdot\boldsymbol{n} \tag{12}$$

where $\boldsymbol{n}$ is a unit vector in the direction of the light propagation. The value of α is 0.5 for the transitions considered but in strained GaAs it can be close to unity [34]. Using (7), (11) and (12) we can write

$$A = -\alpha(T/\tau)\boldsymbol{P}_I\cdot\boldsymbol{n}. \tag{13}$$

It is evident that by measuring A at different positions of the tip above the surface and for light propagating to three non-collinear directions $\boldsymbol{n}_1$, $\boldsymbol{n}_2$ and $\boldsymbol{n}_3$ a complete map of all components of $\boldsymbol{P}_I$ can be obtained (see figure 2). A measurement in only one direction would produce a map of the component of $\boldsymbol{P}_I$ along this particular direction.

To probe the spin polarization of the electrons at the Fermi level its position should be adjusted to be just above the c-band edge of the tip. For p-GaAs this can be done by applying a voltage of about -1.5 V to the sample. Under these circumstances the tunnelling electrons which suffer inelastic scattering (and depolarization) in the sub-surface region of the tip do not have enough energy to reach its interior. Therefore most of the electrons penetrating deep into the tip have traversed this region *ballistically* without loss of their spin polarization.

We assumed above that the kinetic energy of the injected electrons is *low*. However, the case of large band bendings and high bias voltages when the injected electrons are *hot* requires special consideration. Such electrons experience, when propagating along certain directions inside the tip, precession of spin polarization around an effective magnetic field caused by the spin–orbit interaction in conjunction with lack of the inversion symmetry in the III–V compounds [33]. The orientation of this field depends on the direction of the electron quasimomentum $\boldsymbol{k}$. Thus in the bulk the effective magnetic field is randomly oriented due to electron scattering and leads to depolarization of the electrons. However, electrons that are ballistically crossing the band-bending region have momenta with approximately constant direction and all of them feel the same orientation of the effective magnetic field. As a result this field rotates the spin polarization from its initial direction $\boldsymbol{P}_I$ [35]. For GaAs the rotation is maximal for $\boldsymbol{k}\|\langle 110\rangle$ and zero for $\boldsymbol{k}\|\langle 100\rangle$ or $\langle 111\rangle$ [35]. This is because the effective magnetic field is parallel to a vector $\boldsymbol{K}$ with components $K_x = k_x(k_y^2 - k_z^2)$, $K_y = k_y(k_z^2 - k_x^2)$ and $K_z = k_z(k_x^2 - k_y^2)$ in the coordinate frame where the x, y and z axes are directed along $\langle 100\rangle$, $\langle 010\rangle$ and $\langle 001\rangle$, respectively [33]. At low energies of injected electrons the spin precession is small [35], but it may become quite substantial when the electrons gain kinetic energy in a thick band-bending region.

In the experiment with *the ferromagnetic Ni tip and the GaAs sample* photon flux producing 1000 counts s^{-1} in the photomultiplier for each nanoampere of the tunnelling current was observed within a solid angle of $\sim$0.2 sr [5]. The degree of the circular polarization was $\approx -31\%$. In SPSTM where the luminescence is induced in a semiconducting tip instead of a GaAs sample the photon flux may be somewhat lower, requiring the use of single-photon counting techniques. A tip fabricated by selective epitaxial growth, as proposed for an optically pumped SPSTM [17], could provide an effective method for collection of the luminescence radiation. As shown in figure 3 the tip is integrated into an end of a $Ga_{1-(x+\Delta x)}Al_{x+\Delta x}As$–$Ga_{1-x}Al_xAs$–$Ga_{1-(x+\Delta x)}Al_{x+\Delta x}As$ light guide transferring the luminescence to a detector. Such a structure can work as a light guide in this case since the band gap is greater in AlAs (2.14 eV) than in GaAs (1.43 eV) [36]. In this way a single component of $\boldsymbol{P}_I$ can be measured.

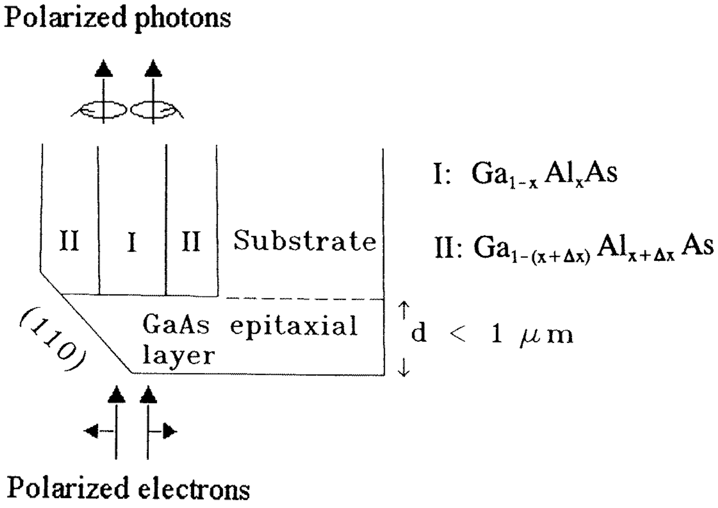

Figure 3. The proposed construction of a GaAs tip integrated into an end of a $Ga_{1-(x+\Delta x)}Al_{x+\Delta x}As$–$Ga_{1-x}Al_xAs$–$Ga_{1-(x+\Delta x)}Al_{x+\Delta x}As$ optical waveguide. The tip apex is formed by a selectively grown GaAs epitaxial layer cleaved at the (110) plane.

3. The local character of the spin polarization

In the model of SPSTM discussed above the magnetic contrast of the image is due to the factor $\boldsymbol{P}_I$ in (13). It depends on the wave functions ψ_σ of the sample side through the tunnelling matrix elements (see (2) and (8)). By applying a bias voltage as shown in figure 1 the Fermi level of the ferromagnet is just above the bulk c-band edge of the semiconductor and thus the energy of the tunnelling electrons is taken to be roughly equal to E_F. In the case of elastic tunnelling of electrons from the sample to the c-band states of the tip these matrix elements have been evaluated in our previous work [17]. The analysis was based on expansion of the tip wave function χ_σ using spherical harmonic components. In the simplest case of a spherically symmetric tip state we can restrict this expansion only to the s-wave. Near the c-band edge of GaAs a linear combination of atomic orbitals (LCAO) wave function with wave vector $\boldsymbol{k} \approx 0$ can be written as

$$\Lambda_c(\boldsymbol{r}) = a \sum_j s(\boldsymbol{r} - \boldsymbol{R}_j) - a' \sum_j s'(\boldsymbol{r} - \boldsymbol{R}'_j). \tag{14}$$

Here $\boldsymbol{R}_j$ ($\boldsymbol{R}'_j$) is the position of the jth cation (anion) where the s-type wave functions, s (s'), are centred and a (a') is a coefficient [37]. In the vacuum outside the tip apex the tail of the wave function has the form

$$\chi_\sigma(\boldsymbol{r}) \propto \mathrm{e}^{\kappa x}/\kappa x \tag{15}$$

where $x = |\boldsymbol{r} - \boldsymbol{r}'|$, $\boldsymbol{r}'$ is the position of the ion at the tip apex and κ is a decay constant of order Å^{-1}. This wave function leads to the relation [17]

$$M_\sigma \propto \psi_\sigma(\boldsymbol{r}') \tag{16}$$

where $\psi_\sigma(\boldsymbol{r}')$ is the sample wave function at the position of the tip apex ion. A similar result was obtained by Tersoff and Hamann [38] in the theory of normal STM. To consider a more general tip wave function Chen's derivative rule [39] can be applied. First we write the angular dependence of the tip wave function in terms of rectangular coordinates x, y and z using a polynomial $Q(x, y, z)$ (for the d_{xy} function, say, $Q(x, y, z) = xy$ etc). Then according to the derivative rule the tunnelling matrix element may be expressed as

$$M_\sigma \propto Q\left(\frac{\partial}{\kappa \partial x'}, \frac{\partial}{\kappa \partial y'}, \frac{\partial}{\kappa \partial z'}\right) \psi_\sigma(\boldsymbol{r}'). \tag{17}$$

Substituting (16) in (8) we obtain

$$P_I = (N_\uparrow |\psi_\uparrow(\boldsymbol{r}')|^2 - N_\downarrow |\psi_\downarrow(\boldsymbol{r}')|^2)/(N_\uparrow |\psi_\uparrow(\boldsymbol{r}')|^2 + N_\downarrow |\psi_\downarrow(\boldsymbol{r}')|^2) \tag{18}$$

where the sample wave functions $\psi_\sigma(\boldsymbol{r}')$ and the density of the state factors correspond to their values at the Fermi level. By definition [17] P_I in (18) is the local degree of spin polarization of the electrons at the point $\boldsymbol{r}'$ and energy E_F. It can be expressed by the ratio of the local spin density $\boldsymbol{m}(\boldsymbol{r}', E_F)$ to the local density of the electronic states of the sample, $\rho_s(\boldsymbol{r}', E_F)$, as

$$P_I = \boldsymbol{m}(\boldsymbol{r}', E_F)/\rho_s(\boldsymbol{r}', E_F). \tag{19}$$

From (13) and (19) we obtain

$$A = -\alpha(T/\tau)[\boldsymbol{m}(\boldsymbol{r}', E_F)/\rho_s(\boldsymbol{r}', E_F)] \cdot \boldsymbol{n}. \tag{20}$$

The magnitudes of $\boldsymbol{P}_I$ and $\boldsymbol{m}$ appear also in the analysis of the spin asymmetry of the tunnelling current flowing between an optically pumped semiconductor tip and a ferromagnetic sample [17]. Thus the effect of the tip in the suggested SPSTM image is reduced to a constant factor ($-\alpha T/\tau$). It is also convenient that, in principle, magnetic contrast is obtained directly without any supplementary procedure.

It has been suggested [40] that predominantly s–d-hybridized bands with nearly spherical Fermi surface contribute to the tunnelling current from a transition metal ferromagnet (Co, Fe, Ni) and that the electron effective mass is close to the free electron mass. Using this model and the approximation of a rectangular potential barrier with corresponding wave functions [41] we obtain from (18)

$$P_I = (\kappa^2 - k_\uparrow k_\downarrow)(k_\uparrow - k_\downarrow)/(\kappa^2 + k_\uparrow k_\downarrow)(k_\uparrow + k_\downarrow) \tag{21}$$

where k_σ is the Fermi momentum of a σ-electron. Due to the factor $\kappa^2 - k_\uparrow k_\downarrow$ the spin polarization can change its sign although the bulk polarization $P_b = (k_\uparrow - k_\downarrow)/(k_\uparrow + k_\downarrow)$ is always positive. For instance, the values of P_I are 17 and -2% when calculated from (21) for Fe and Ni using the barrier height of 4 eV and the Fermi momenta [40] $k_\uparrow = 1.10$ and $k_\downarrow = 0.42$ for Fe and $k_\uparrow = 1.16$ and $k_\downarrow = 0.95$ for Ni in the units of Å^{-1}, respectively.

It should be noted that the Bardeen theory is valid for slow tunnelling rates, requiring that $\exp(-\kappa \mathrm{d}) \ll 1$ where d is the width of the barrier. At intermediate rates a more precise treatment is needed. In the case of a rectangular barrier the exact solution of the tunnelling problem [42] can be used. Then we obtain the spin polarization as a function of κd in the form

$$P_I(\kappa d) = [\sinh^2(\kappa d)(\kappa^2 - k_\uparrow k_\downarrow) + k_\uparrow k_\downarrow](k_\uparrow - k_\downarrow)/[\sinh^2(\kappa d)(\kappa^2 + k_\uparrow k_\downarrow) + k_\uparrow k_\downarrow](k_\uparrow + k_\downarrow). \tag{22}$$

When κd is increased from zero to infinity $P_I(\kappa d)$ ranges from the bulk value $P_b = (k_\uparrow - k_\downarrow)/(k_\uparrow + k_\downarrow)$ to that of P_I in (21) as shown in figure 4 in the case of Ni (the results for Fe and Co are very similar). Other features of P_I are that for a wide ($\sinh^2(\kappa d) \gg 1$) but low ($\kappa^2 \ll k_\uparrow k_\downarrow$) barrier $P_I = -P_b$ and that for any values of κ, d, $k_\uparrow$ and $k_\downarrow$ it is between P_b and $-P_b$.

According to calculations [11] $\boldsymbol{P_I}$ is sensitive to the shape of the spin-dependent tunnelling barrier potential. The barrier between the sample and the tip is not rectangular because a negative bias voltage (about -1.5 V in GaAs) is needed to raise the Fermi level of the (ferromagnetic) specimen above the semiconductor's c-band edge. A trapezoidal barrier shape would be more realistic (see figure 1) to handle the problem. Inside the barrier region the wave function can be expressed [43] as a linear combination of Airy functions Ai(ξ) and Bi(ξ) with

$$\xi = (2m_e/\hbar^2)^{1/3}[\phi(d/(\phi - \varphi + eV))^{2/3} - ((\phi - \varphi + eV)/d)^{1/3}x]. \tag{23}$$

Here ϕ and φ are the work functions of the ferromagnet and the semiconductor, respectively. However, it is found that with a bias voltage of the order of -1.4 V the value of $\boldsymbol{P_I}$ is nearly the same as for the rectangular barrier.

In STM experiments the apparent barrier height is frequently lower (even 1 eV or less) than the work function of the tip and the sample materials. In this case the negative polarization of Ni can be close to its limit $-10\% = -P_b$ (see the discussion after (22)). It is well known that different measuring methods give very different polarization values for the same material [5, 44–46]. In tunnelling experiments using an Ni STM tip and GaAs sample a negative polarization with maximum value of $P = (-31 \pm 5.6)\%$ was observed [5]. On the other hand electron-capture spectroscopy of Ni surfaces [44] reveals very high negative Fermi-level polarization, up to -95%. Tunnelling measurements between a thin superconductor Al film and a thin polycrystalline Ni film give a positive polarization (11%) close to the bulk value (10%) [45]. Low negative polarizations (<-5%) that are

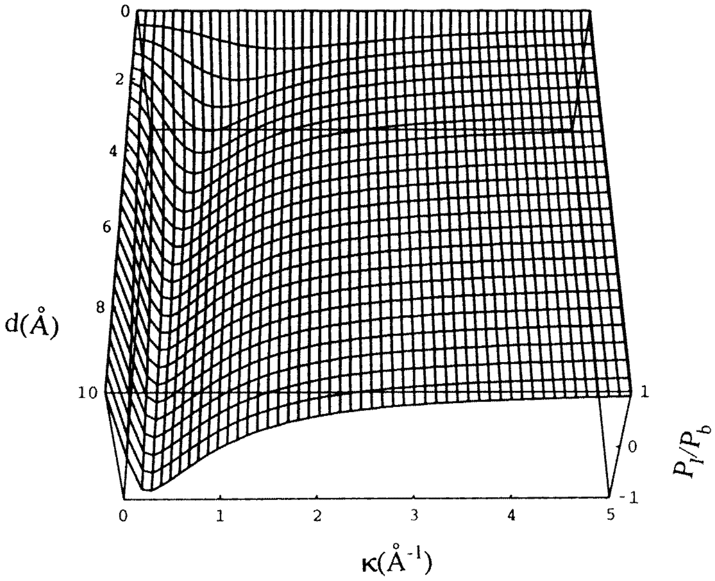

Figure 4. Calculated degree of the spin polarization P_I of electrons tunnelling from Ni into a GaAs tip as a function of the tip–sample separation (d) and the surface wave function decay constant (κ). P_I is normalized against the bulk polarization (P_b). A rectangular tunnelling barrier is assumed. For a sufficiently wide barrier ($d \geqslant 10$ Å) P_I changes rapidly from $-P_b$ to $+P_b$ when κ is reduced to near zero.

close to those given by (21) with reasonable values of κ were found on Ni surfaces using spin-polarized field emission experiments [46].

The value of P depends on the bias voltage [5]. The maximum degree of negative polarization was found while the Fermi level of the ferromagnet (Ni) was just above the c-band edge of the GaAs sample, corresponding to a voltage of about -1.5 V applied to the ferromagnetic tip. At higher voltages it seems that P oscillates, attaining a minimum at about -2.2 V and a maximum at -2.5 V. Such behaviour could be explained by assuming a spin-dependent potential at the Ni surface [47, 48]. The theory set forth in [47] and [48] indicates that the effective surface potential barrier is lower for the minority spin electrons. As a result these electrons have greater tunnelling probability, which explains the high negative polarization found in the experiments [5]. For a biased tip (Ni) and sample (GaAs) the barrier is approximately triangular with deeper inclination for the majority spin electrons. When the negative voltage on Ni is increased the relative difference between the potential barriers for the electrons with up and down spins will diminish, reducing thus the negative polarization of the tunnelling current of the Fermi level electrons. For the same reason the tunnelling current which originates from the states below the Fermi level of the Ni tip is even less negatively polarized. Possible depolarization due to scattering in the band-bending region will further reduce the spin polarization.

At sufficiently high voltages part of the barrier near the GaAs surface becomes classically accessible (Fowler–Nordheim regime [49]). When this area is wide enough the interference of transmitted and reflected electrons causes well known surface resonances [49, 50] localized at the GaAs surface. Their appearance will enhance the transfer of electrons through the barrier and can be seen as a sequence of oscillations in the tunnelling conductance (Gundlach oscillations [50]). In our case the classically accessible part of the barrier is wider for the minority spin electrons and thus the first peak of the conductance can be attributed to them. This may explain the maximum of the negative polarization seen in the experiment [5]. On the other hand the voltage corresponding to this maximum is in the range where the Gundlach oscillations were found in STM experiments at the Ni surface [51]. We are planning to investigate this hypothesis. On the other hand further experimental studies of such oscillations of the polarization of tunnelling electrons would help to investigate the spin-dependent potential of magnetically ordered surfaces, a question which is crucial for understanding SPSTM.

4. Conclusions

STM based on detection of the degree of circular polarization of luminescence radiation (A) created in a GaAs tip as a result of recombination of spin-polarized electrons transferred from a magnetic sample is analysed.

Using the Bardeen transfer-Hamiltonian method we show that measurements of A for radiation propagating in three non-collinear directions can provide a map of the local electronic spin polarization vector of the sample surface, probably with subnanometre resolution. In this method it is unnecessary to alter the sample polarization in order to obtain magnetic contrast in the STM image, a circumstance that is a major drawback when using a ferromagnetic tip in a spin-sensitive STM [4, 6]. Because a non-magnetic semiconductor tip is used the method analysed here can be considered as non-destructive with respect to surface magnetization.

It is expected that for electron injection energies just above the bottom of the c-band of the tip the spin-polarized electrons tunnelling from the sample traverse the band-bending region *ballistically*. Thus the sub-surface region has only a small effect on the ESP of the injected electrons.

The STM experiments should be carried out under ultra high vacuum (UHV) because non-crystalline native oxide layer on a GaAs tip reduces spin-polarized electron transfer from the sample to the bulk of the tip. However, the tip can be prepared in air, cleaving it from a single-crystal GaAs wafer and removing the oxide layer afterwards inside the UHV chamber with hydrogen plasma treatment. UHV is necessary also because the electron spin polarization of the sample surface is sensitive to contamination. Recent experiments on GaAs tips which have been passivated with sulphur atoms are quite interesting because the tip can work even under ambient pressure [52]. The band-bending region introduced in such a case would not necessarily influence too severely the electrons traversing this region ballistically.

References

[1] Binnig G, Rohrer H, Gerber Ch and Weibel E 1982 *Phys. Rev. Lett.* **49** 57
[2] Binnig G, Quate C F and Gerber Ch 1986 *Phys. Rev. Lett.* **56** 930
[3] Minakov A A and Shvets I V 1990 *Surf. Sci.* **236** L377
[4] Wiesendanger R, Güntherodt H-J, Güntherodt G, Gambino R J and Ruf R 1990 *Phys. Rev. Lett.* **65** 247
[5] Alvarado S F and Renaud P 1992 *Phys. Rev. Lett.* **68** 1387
[6] Wiesendanger R, Shvets I V, Bürgler D, Tarrach G, Güntherodt H-J and Coey J M D 1992 *Europhys. Lett.* **19** 141
[7] Molotkov S N 1992 *Pis. Zh. Eksp. Teor. Fiz.* **55** 180
[8] Laiho R and Reittu H J 1993 *Surf. Sci.* **289** 363
[9] Sueoka K, Mukasa K and Hayakawa K 1993 *Japan. J. Appl. Phys.* **32** 2989
[10] Nunes G Jr and Amer N M 1993 *Appl. Phys. Lett.* **63** 1851

[11] Reittu H J 1994 *J. Phys.: Condens. Matter* **6** 1847

[12] Jansen R, van der Wielen M C M M, Prins M W J, Abraham D L and van Kempen H 1994 *J. Vac. Sci. Technol.* B **12** 2133

[13] Manassen Y 1994 *Adv. Mater.* **6** 401

[14] Yamaguchi K, Okamoto K and Yugo S 1995 *J. Appl. Phys.* **77** 6061

[15] Prins M W J, van Kempen H, van Leuken H, de Groot R A, Van Roy W and De Boeck J 1995 *J. Phys.: Condens. Matter* **7** 9447

[16] Reittu H J 1995 *Surf. Sci.* **334** 257

[17] Laiho R and Reittu H 1996 *Fiz. Tverd. Tela* **38** 918 (Engl. Trans. 1996 *Sov. Phys. Solid State* **38** 506)

[18] Martin Y and Wickramasinghe H K 1987 *Appl. Phys. Lett.* **50** 1455

[19] Saenz J J, Garcia N, Grütter P, Meyer E, Heinzelmann H, Wiesendanger R, Rosenthaler L, Hidber H R and Güntherodt H-J 1987 *J. Appl. Phys.* **62** 4293

[20] Prins M W J, Groeneveld R H M, Abraham D L, van Kempen H and van Kesteren H W 1995 *Appl. Phys. Lett.* **66** 1141

[21] Slonczewski J C 1989 *Phys. Rev.* B **39** 6995

[22] Prins M W J, Abraham D L and van Kempen H 1993 *J. Magn. Magn. Mater.* **121** 152

[23] Pierce D T and Celotta R J 1984 *Optical Orientation* ed F Meier and B P Zakharchenya (Amsterdam: North-Holland) p 260

[24] Hecht M H 1990 *Phys. Rev.* B **41** 7918

[25] Coombs J H, Gimzewski J K, Reihl B, Sass J K and Schlittler R R 1988 *J. Microsc.* **152** 325

[26] Abraham D L, Veider A, Schönenberger Ch, Meier H P, Arent D J and Alvarado S F 1990 *Appl. Phys. Lett.* **56** 1564

[27] Johansson P, Monreal R and Appel P 1990 *Phys. Rev.* B **42** 42

[28] Johansson P and Monreal M 1991 *Z. Phys.* B **84** 269

[29] Majlis N, Yeyati A L, Flores F and Monreal R 1995 *Phys. Rev.* B **52** 12 505

[30] Vazques de Parga A L and Alvarado S F 1994 *Phys. Rev. Lett.* **72** 3726

[31] Molotkov S N 1996 *Phys. Low-Dim. Struct.* **1/2** 47

[32] Bardeen J 1961 *Phys. Rev. Lett.* **6** 57

[33] Dyakonov M I and Perel V I 1984 *Optical Orientation* ed F Meier and B P Zakharchenya (Amsterdam: North-Holland) p 11

[34] Nakanishi T, Aoyagi H, Horinaka H, Kamiya Y, Kato T, Nakamura S, Saka T and Tsubata M 1991 *Phys. Lett.* **158A** 345

[35] Riechert H, Alvarado S F, Titkov A N and Safarov V I 1984 *Phys. Rev. Lett.* **52** 2297

[36] *Landolt–Börnstein New Series* 1982 vol 17a, ed O Madelung (Berlin: Springer)

[37] Hermann C and Weisbuch C 1984 *Optical Orientation* ed F Meier and B P Zakharchenya (Amsterdam: North-Holland) p 463

[38] Tersoff J and Hamann D R 1985 *Phys. Rev.* B **31** 805

[39] Chen C J 1993 *Introduction to Scanning Tunnelling Microscopy* (New York: Oxford University Press) p 75

[40] Stearns M B 1977 *J. Magn. Magn. Mater.* **5** 167

[41] Reittu H J 1995 *Am. J. Phys.* **63** 940

[42] Landau L D and Lifshitz E M 1958 *Quantum Mechanics: Nonrelativistic Theory* (Oxford: Pergamon) p 72

[43] Yu P Y and Cardona M 1996 *Fundamentals of Semiconductors* (Berlin: Springer) p 313

[44] Rau C and Eichner S 1981 *Phys. Rev. Lett.* **47** 939
Rau C 1982 *J. Magn. Magn. Mater.* **30** 141

[45] Tedrow P M and Meservey R 1973 *Phys. Rev.* B **7** 318

[46] Landolt M and Campagna M 1977 *Phys. Rev. Lett.* **38** 663

[47] Nagy D 1979 *Surf. Sci.* **90** 102

[48] Nagy D, Cutler P H and Feuchtwang T E 1979 *Phys. Rev.* B **19** 2964

[49] Wolf E L 1985 *Principles of Electron Tunnelling Spectroscopy* (New York: Oxford University Press) pp 62–8

[50] Gundlach K H 1966 *Solid State Electron* **9** 949

[51] Binnig G, Frank K H, Fuchs H, Garcia N, Reihl B, Rohrer H, Salvan F and Williams A R 1985 *Phys. Rev. Lett.* **55** 991

[52] Yamaguchi K and Tada S 1996 *J. Electrochem. Soc.* **143** 2616